J. Appl. Environ. Biol. Sci., 5(8S)594-603, 2015

ISSN: 2090-4274
Journal of Applied Environmental and Biological Sciences
www.textroad.com

Electrical Impedance Tomography System to Circumstances Recognition of Tissue in an Experimental Phantom: Tooth a Case Study

Seyed Masoud Zargari[1], Zahra Vahabi[2],Rassoul Amifattahi[2], Mahdi Vahabi[3] and Ebrahim Ahmadifard[4]

[1]Department of Electrical Engineering , Islamic Azad University of Najaf Abad, Isfahan, Iran
[2]Digital Signal Processing Research Lab, Department of Electrical and Computer Engineering, Isfahan University of Technology, Isfahan, 84156-83111, Iran
[3] Mechanical Engineering Department, AmirKabir University of Technology
[4]Ragheb Institute

Received: March 8, 2015
Accepted: May 10, 2015

ABSTRACT

Up to now, several methods for the location of the root of the tooth and calculating the tooth decay detection is presented, such as the statistical use of the teeth length mean, using feeling of hand and radiography.
The most important and most valuable developments in dentistry and endodontic, is the discovery of anesthesia and the use of X-ray and radiography.
Common method to determine the root of tooth is to providing films; but in some cases may provide a suitable radiography is not feasible due to problems such as nausea, severe reaction, pregnancy, etc. On the other hand the dangers of radiation, particularly in children and radiological problems in people with disabilities, disadvantaged and our children on this thinking that if a device can determine the root caries detection, and effectively used instead of X-ray radiation levels reduce the radiation to the patient, will be valuable and this led to the idea of electronic instruments and determine root caries detection using impedance measurements.

KEYWORDS: current source, dental decay, experimental measurement, impedance tomography, multi frequency, root position

1-INTRODUCTION

The most important and most valuabledevelopments in dentistry and endodontic, is the discovery of anesthesia and the use of X-ray and X-ray.[1] Apex Finder or Root Finder [2-3] is a device that determined root length with high precision to the tenth of a millimeter to prevent short or long root filling. We all are familiar to issues of the treatment of partial canal; one of these devices that can reduce such problems is the Root Finder device.[1-4-5]

Tooth decay is the most common cause of tooth loss.Early detection of decay is a major step in preventing tooth decay that is caused by injury.[6] Tooth decay irreversible stage is the process of decay-causing bacteria acid soluble minerals (mainly Streptococcus mutants), and treatment is the only way to replace the lost hard tissue of teeth with dental restorative materials.

If tooth decay is not replaced in time and stop tooth decay reaches the nerve root canal treatment is needed in severe cases may lead to tooth extraction.[7]

Performance of the system is by electrodes to flow into the gums and impedance measuring points and points where impedance is less difficult in the areas of tissue such as root rot has occurred there or on the gums.[8-9]

Of course, for the detection of tooth decay, surface electrodes are put on the crown.

Tissue resistance depends to factors such as the location of the touch, the touch surface, the entrance and exit of flow, the flow rate, a flow of current, voltage, and the difficulty of electrode connection to the skin.

You can see the block diagram of the electronic system (impedance journalist) in (Figure 1).

Corresponding author: Zahra Vahabi, Department of Electrical and Computer Engineering, Isfahan University of Technology, Isfahan, 84156-83111, Iran. S.masoud.zargari@gmail.com

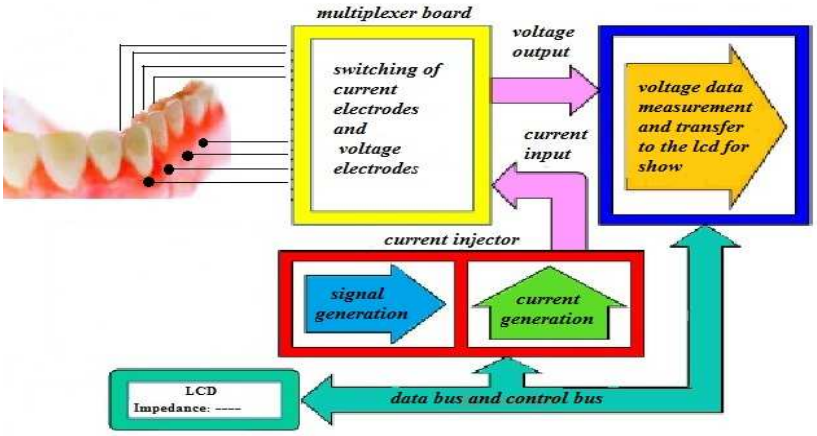

Figure 1: Block diagram of the system impedance journalist.

2- MATERIALS AND METHODS

2-1-Electrical Impedance Tomography (EIT)

Electrical Impedance Tomography (EIT); is an inexpensive and fast non-invasive imaging technique.
This technique with measurements of the surface of an object and with a non-destructive and non-invasive method; achieves internal impedance distribution of desired object.
In this system, a number of electrodes is installed on the surface of the target object and a few tens of kHz sinusoidal current is applied to one or more pairs of electrodes of and voltage of other pairs of electrodes that act as sensors measured.
Electrical impedance tomography theory is that by applying a constant current through a material, voltage distribution formed on the surface of the material will reflect the internal distribution of resistivity.
Of course, we know that several different resistance distributions can produce a voltage distribution equal level [10-14].
So this system simulates in many ways until limit resistance distribution. (Figure 2) is a simplified diagram of the EIT with 16 electrodes on the circumference of a circle in this current system l applied between a pair of electrodes on opposite sides of the core; at the same time, the voltage distribution VI measures between the two adjacent electrodes.
After the voltage was measured in the whole environment, the stimulating electrodes rotate to adjacent electrodes, so that still remain opposed, and the voltage across the electrodes is again measured. This process continues until full voltage to be measured 256 series.[10-14-15-16]

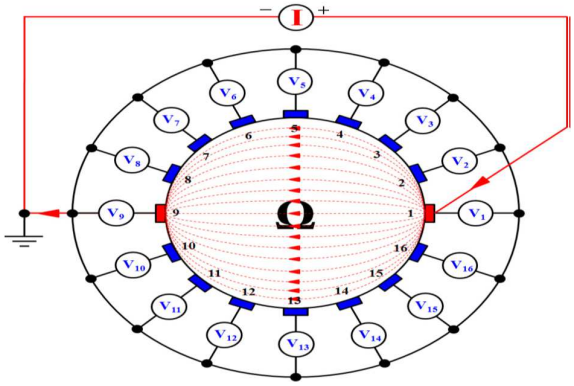

Figure 2: Diagram of the test 16 electrodes EIT.

The magnetic and electrical fields Time - Harmony can mention equations (1,2) .

$\varepsilon(x,t) = Re\ \{E(x, w)e^{iwt}$ (1)

$H(x,t) = Re\ \{H(x,w)\ e^{iwt}$ (2)

In equations (3,4) makes Maxwell

$\nabla * H(x , w) = \gamma(x , w) E(x , w)$ (3)

$\nabla * E(x , w) = -iw\mu (x)H (x,w)$ (4)

The μ (X) is the Trojan or permeability and Re {F} implies real part of a complex function F.[11-12-13]

EIT at low frequencies ω acts coordinate with | ɣ | and length scale L that ωμ L ^ 2 << 1 so after simple analysis of the scale and above equation in equation (5) is estimated to be:

$\nabla * E(x , w) = 0$ (5)

Electric potential ϕ define and the vector and current density of time – harmony has been show in the relationships (6,7,8):

$\nabla * E (x,w) = - \nabla \phi (x,w)$ (6)

$\nabla * H(x,w)=j(x,w)$ (7)

$j(x)= - \Upsilon(x,w)\nabla\phi(x,w)$ (8)

Note that the energy density over time swings the equation (9):

$$\frac{w}{2\pi}\int_{t}^{t+\frac{\pi}{w}} I(x,\tau)\,.\,\varepsilon(x,\tau)d\tau = \frac{1}{2}[Re\{j(x,w)\}.Re\{E(x,w)\} + Im\{j(x,w)\}\,.\,Im\{E(x,w)\}] = \frac{1}{2}\sigma(x)\,\big|\,\nabla\emptyset(x,w)\,\big| \quad (9)$$

And must be a positive value, so that the equation (10) is observed:

$\sigma(x) = Re\{\gamma(x,w)\} \geq m > 0$ (10)

The majority of results in materials with permeability isotropic ɣ (x, ω) and function scale (Ω) L ^ ∞ show that Ω is a domain.[17-18]

2-2- Multi-frequency current source

Multi-frequency current source (Figure 6) is developed with a minimum number of parts with low cost. This circuit formed of an oscillator of a variable frequency voltage (Figure 3) VCO(Voltage Controlled Oscillator) and a controlled current source of modified Howland (Figure 4) VCCS (modified Howland Voltage Control Current Source)[19].

VCO that is developed and high-frequency, is precision generator IC function, MAX038, and linked to a minimum of elements that are not product energy for circuit. VCO provides signals with different frequency bandwidth that depends on the amount of capacitance C_f. VCO frequency is a function of the output power supply voltage with a positive $R_{in}$and C_fDC, 5 ± volts[20] .

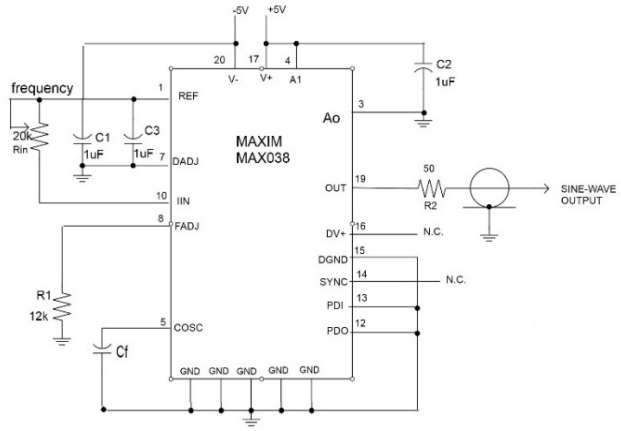

Figure 3: a voltage controlled oscillator (VCO) with IC MAX038

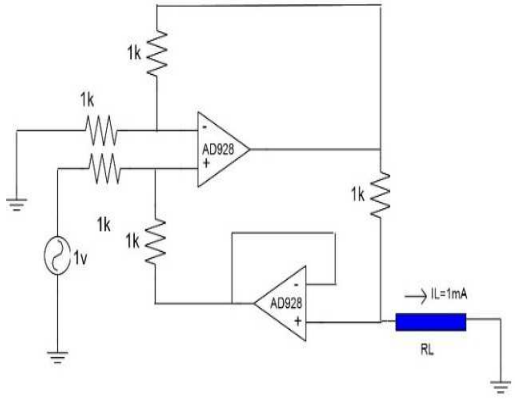

Figure 4: based on the modified circuit Howland VCCS.

$C_f$connected to a particular frequency capacitor, such as a single-pole signal using DIP switch is used with a certain amount of R_{in}. Sinusoidal voltage signal of very high bandwidth obtained from the VCO output of VCCS is fed to a generator modified Howland current[21-25-26].

Nine different capacitor (figure 5-B) are connected for variable broadband separately.

As in (Figure 5-A) can be seen in this article 1khz to 15khz frequency used that the capacitor equivalent to 33nf $C_f$about 1µf is needed.

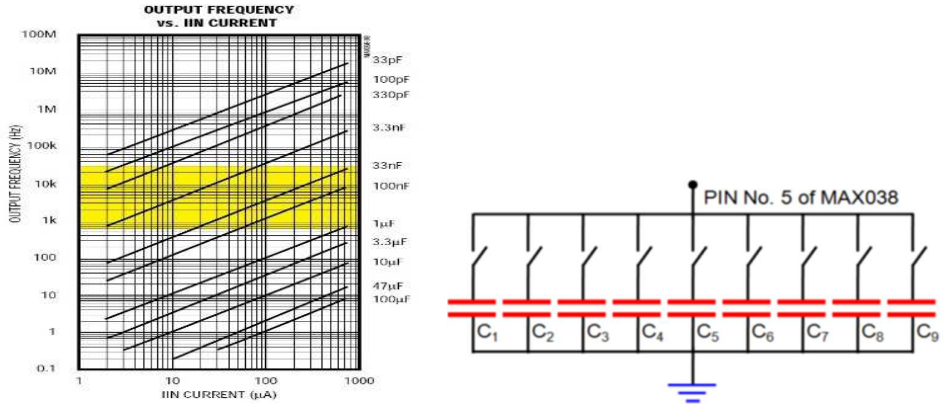

(a) (b)

Figure 5: (a) capacitors of different frequency band IC MAX038 (b) capacitor banks for different frequency bands[19-20].

Output VCO, F_O (Figure3) from equation (11) is obtained[20]:

$$F_O = \frac{2\times 2.5V}{R_{in}\times C_f} \qquad (11)$$

VCCS has been developed with an IC, AD829. This IC has extremely low noise and a high-speed provides Op-Amp that user interest in the preservation of 20 ± 1 ± has a better bandwidth of 50 kHz. An output of a constant current converter amplifier connected to alternate between VCO and VCCS for VCO control voltage. VCCS output loads with 1 kilo-ohm resistance and it can be seen that the output voltage remains constant during the period 1 kilo- ohm load resistance is greater than 1 MHz. VCCS represents the frequency obtained from maintaining a constant current in the load circuit is above 1MHz[22-23-27].

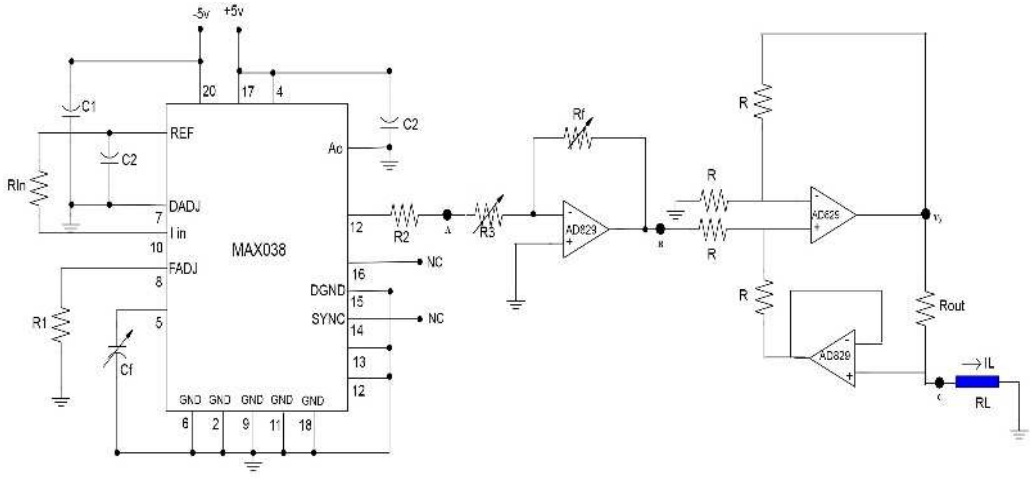

Figure 6: Multi-frequency current source.

The block diagram (Figure 6) observed that max038 IC output at 10 Hz frequency up to 10 MHz as a sine wave is produced. The use of amplifiers and AD829 IC is because of long distance and we do not have a drop in voltage and current. The strengthening is obtained of the relationship between the outputs voltages divided by the input voltage. The output current of the circuit (Figure 4) is calculated in equations (12,13,14,15) and the calculations can get the output you need.

$$V^+ = \frac{V_I}{2} + \frac{V_O}{2} \quad (12)$$

$$V_Y = \left(1 + \frac{R}{R}\right)\left[\frac{V_I}{2} + \frac{V_O}{2}\right] = V_I + V_0 \quad (13)$$

$$I_L = \frac{V_Y - V_O}{R_{OUT}} = \frac{V_I + V_O - V_O}{R_{OUT}} = \frac{V_I}{R_{OUT}} \quad (14)$$

$$I_L = \frac{V_I}{R_{OUT}} \quad (15)$$

Of the circuit (Figure 6) using equations (16,17) can be output

$$V_B = -V_A\left(\frac{R_f}{R_3}\right) \quad (16)$$

$$I_L = \frac{V_B}{R_{OUT}} \quad (17)$$

After injecting the current by electrodes to the tissue strengthen the desired voltage obtained from the tissues, and controls notch filter and give to the Micro and display impedance on the LCD.

To boost the voltage across tissue use instrumentation amplifier that has low noise the amplifier (Figure 7) with great accuracy and stability are required for long-term circuits and short circuits[24].

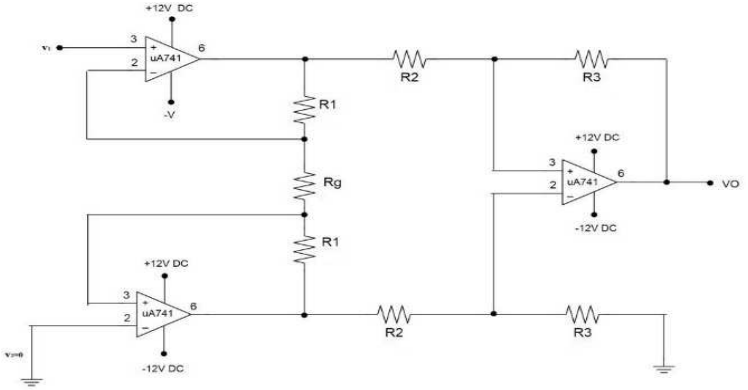

Figure 7: instrumentation amplifier circuit with three IC 741.

Amplified voltage to the micro level and measuring voltage and, display the impedance of the tissue on the LCD.

3- RESULTS AND DISCUSSION

The obtained output of variable frequency voltage oscillator circuit from 1 kHz to 10 kHz frequency VCO used in this article. VCO output signal is at a desired frequency regardless of

the frequency noise; so it's suitable for the multi frequency EIT studies. VCO frequency response as the output voltage remains constant and is very acceptable over a wide frequency band. The frequency response of VCO (Figure 8) as an acceptable voltage (1000mv) the time remaining between the frequencies of 10 Hz to 1 MHz is 1kΩ. In (Figure 8) can be seen in 1 kHz to 15 kHz frequency used in this article, as well as when it contains 100 kHz frequency voltage is acceptable 1000mv contains stability and is suitable for EIT experiments.

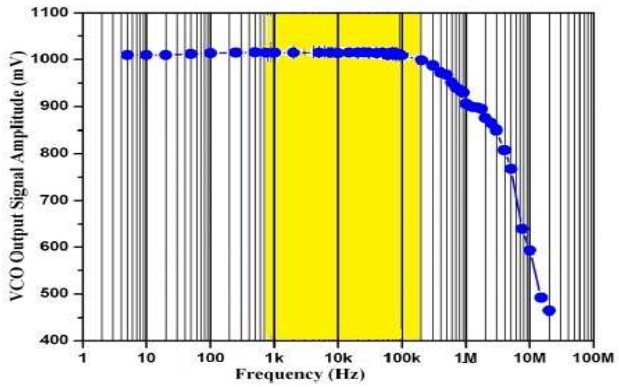

Figure 8: VCO frequency response.

Voltage reduction and better accuracy at higher frequencies.

5kΩ to 10 kHz frequency impedance measurements in the diagram (Figure 9) is observed. 5KΩ expected results with results at higher frequencies, is closer.

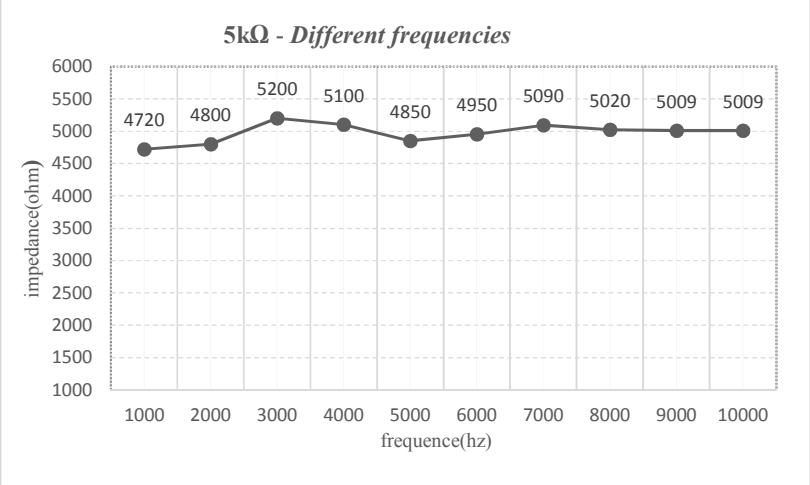

Figure 9: Figure 5 k Ω impedance at frequencies up to 10 kHz.

As can be seen in the charts above high-frequency measured value is closer to the desired value. Phantom EIT (Figure 10) that consists of a set of sixteen electrodes the electrodes made of stainless steel with equal distance from the center of the tooth As well as each of the electrodes apart from each other are the same. 100% of the plastic tank and a short wall (shallow reservoir) are used as the reservoir is filled with a solution of KCL.

Figure 10: PhantomEITwith16electrode

Table 1: Measurement ofsix healthyteethand sixdentaldecay,six surface and deeptoothdecay

	Impedance(kΩ)		
Test	*Healthy Teeth*	*Superficial Caries*	*Deep Caries*
Test 1	**1.01**	**3.15**	**14.20**
Test 2	**1.96**	**3.71**	**16.51**
Test 3	**2.32**	**5.23**	**18.02**
Test 4	**0.95**	**5.81**	**18.34**
Test 5	**1.52**	**4.01**	**15.11**
Test 6	**2.02**	**3.95**	**14.82**
Average ($\bar{x}$)	**1.63**	**4.31**	**16.16**
Variance (σ^2)	**0.3192**	**0.94632**	**3.01484**

Table 2: Results of measurements ofteethtest1.

Test1 healthy teeth - Different Frequencies										
Frequency(khz)	**1**	**2**	**3**	**4**	**5**	**6**	**7**	**8**	**9**	**10**
impedance(kΩ)	**13.75**	**13.76**	**13.81**	**13.88**	**13.92**	**14.01**	**14.18**	**14.20**	**14.20**	**14.20**

According to the tests conducted on six healthy teeth and six tooth decay in the enamel and dentin and six others on the neck of tooth decay deep 10khz frequency and the amount of results has shown in Table 1.
The diagram (Figure 11) shows the curve of results in Table 1.

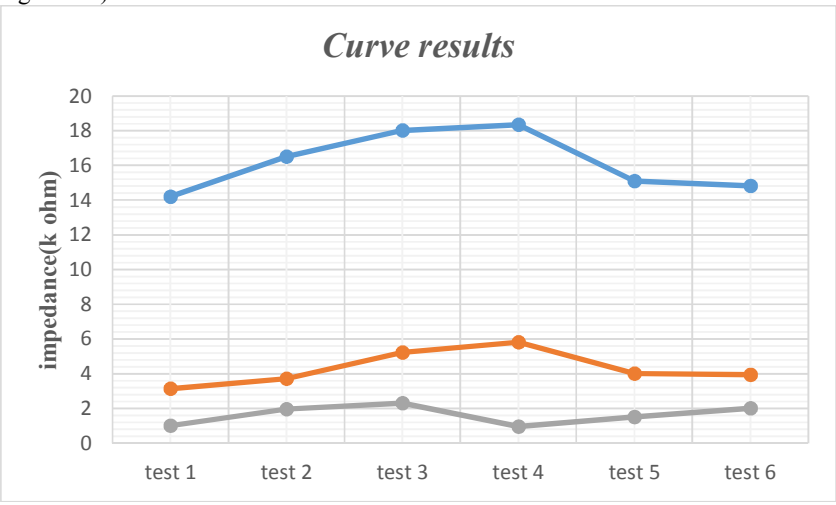

Figure 11: Chart from Table 1(Blue for Deep Caries, Red for Superficial Caries and Gray for Healthy).

As mentioned increase of safety is according to the voltage loss and better accuracy is at higher frequencies so test test1 for healthy teeth in frenquency of the 1khz to 10khz repeat again and the results are visible in Table 2.

By observing the chart (Figure 12), which is obtained from Table 2, we know that at high frequencies the expected results are closer to the obtained results.

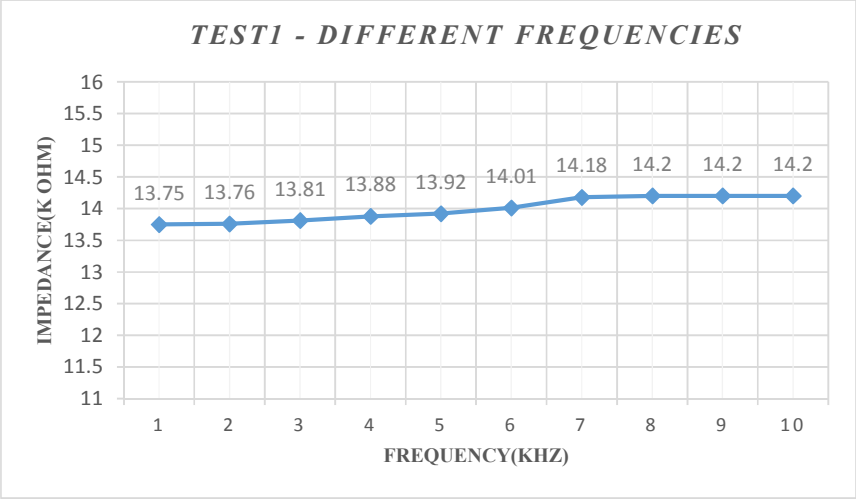

Figure 12: Chart from Table 2.

Samples of healthy and decayed teeth that have cavities on the surface and depth have been tested are visible in (Figure 13).

Table 3 : Average of teeth and decay of teeth

Average Electrical Parameters	
Electrical parameters	**Impedance(kΩ)**
Healthy Teeth	***1.63±1.01***
Superficial Caries	***4.31±2.22***
Deep Caries	***16.16±2.18***

Figure 13: Healthyandrottenteeth

See Tables 1 and observing carefully average three types of healthy teeth , decay, surface and deep cavities in teeth decay we know that impedance tooth decay deep below the surface , and the impedance of both decay of teeth less than healthy teeth.

Table 3 Average impedance teeth , tooth decay and tooth decay deep level with the amount of error is calculated and evaluated .

The journalist impedance measurement system (Figure 14) specifies the subject that how deep the root decay the lower impedance You can also use this system to get the root location of teeth .

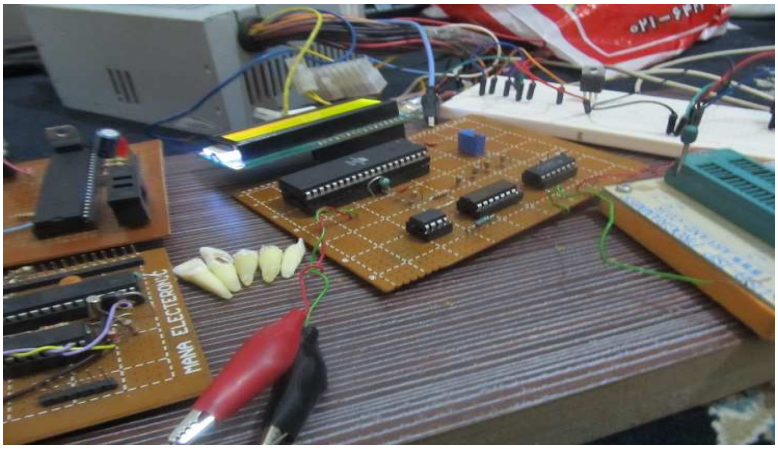

Figure 14 : Experiments with impedance journalist.

The diagram (Figure 15) is related to the results of Table .

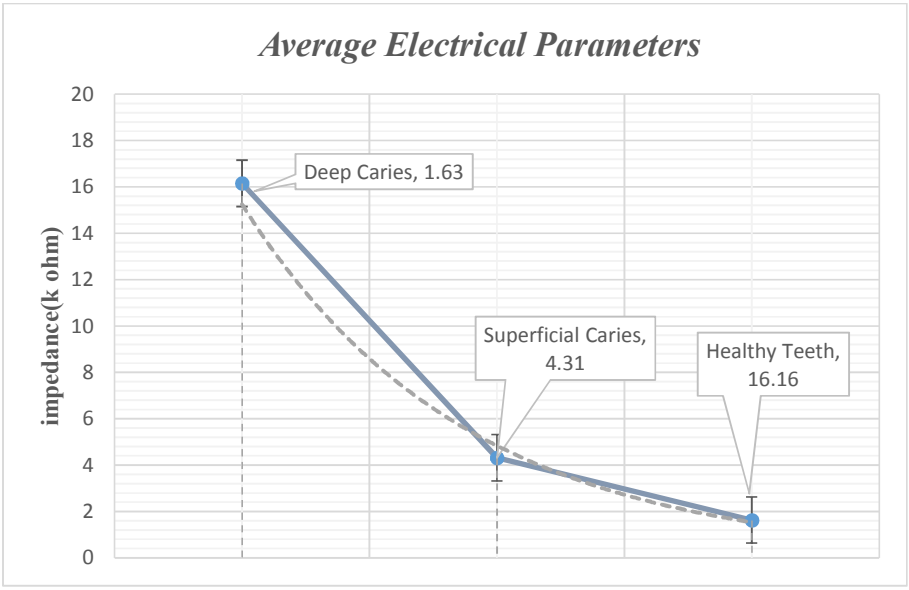

3 .

Figure 15: The relationship between tooth decay and resistance.

4- CONCLUSION

Multi- frequency current source developed with a minimal number of parts suitable for applications with low cost and high bandwidth EIT (10HZ-10MHZ).

As was seen in the graph resistance rate changes with decay rate and decreases by the electrical resistance increase.

Thus, according to the results of the use of these electrical parameters can be a useful tool for diagnosis especially in the treatment of deep caries, root rot, and is recommended as a good method for caries detection depth as well as to determine the root location of the results.

REFERENCES

[1] S. Cohen, R. C.Burns. "Pathways of the pulp,"7 th ed,Missouri, Mosby. 1997; 209.

[2] D. H.pratten, N. J. McDonald. "Comparison of radiographic and electronic working lenghts. "J Endodon, 1996; 22(4),pp. 173-6.

[3] Y. Nahmias,J. A.Aurelio,H.Gerstein. "Expanded use of the electronic canal length measuring devices.", J Endodon, 1983 ;9(8),pp:347-9.

[4]M. Mesgarpour , "Technology dental equipment,", Wide Word Publications,2012.

[5]J. Cameron, R. john , Medical Physics , Publications Yyzh , 2008.

[6] S. Twetman, S. Axelsson, G.Dahlén, I.Espelid, Mejàre,I. Norlund A. "Adjunct methods for caries detection: A systematic review of literature.", Acta Odontologica Scandinavica 2013;71(3-4), pp.388-97.

[7] T. Roberson, H. O.Heymann, E. J.Swift. "Sturdevant's art and science of operative dentistry", Elsevier Health Sciences; 2006, 12(2), pp.260-300.

[8] M. Paunovic and M. Schlesinger," Fundamentals of Electrochemical Deposition, The Electrochemical Society Series.", 2nd Ed., John Wiley &Sons, Inc, 2006.

[9] M. Gad-el-Hak, "The MEMS Handbook The Mechanical Engineering Handbook Series." , CRC Press Boca Raton London New York Washington, D.C, Chapter-16, Sec. 16.16.3,2010.

[10] P.Metherall,"Three Dimensional Electrical Impedance Tomography of the Human Thorax." , PhD Thesis, University of Sheffield. Jan' 1998.

[11] T. KBera. ,J.Nagaraju, "A Reconfigurable Practical Phantom for Studying the 2-D Electrical Impedance Tomography (EIT) Using a FEM Based Forward Solver." , Online Proceedings of 10th International Conference on Biomedical Applications of Electrical Impedance Tomography (EIT 2009), School of Mathematics, The University of Manchester, UK, 16th-19th June 2009.

[12] T. J. Yorkey , "Comparing reconstruction methods for electrical impedance tomography.", PhD thesis, University of Wisconsin at Madison, Madison, WI 53706, 1986

[13] B. M.Graham, "Enhancements in Electrical Impedance Tomography (EIT) Image Reconstruction for 3D Lung Imaging." , PhD thesis, University of Ottawa, April 2007.

[14] L. Borcea, "Computational and Applied Mathematics.", MS 134, Rice University, 6100 Main Street, Houston, USA,1892, TX 77005.

[15] G. Beylkin ,"The inversion problem and applications of the generalized Radon transform Commun." , Pure Appl,1984,Math. 37(2), pp. 580-92.

[16] F. Santosa ,M. A."Vogelius ,backprojection algorithm for electrical impedance imaging.", SIAM J. Appl, 1990 Math. 50, pp. 216–4399.

[17] D. Isaacson,M. Cheney ,"Effects of measurement precision and finite number of electrodes on linear impedance imaging algorithms.", SIAM J. Appl. 2001, Math. 12(3), pp. 1705–31.

[18] M. Cheney, D. Isaacson ,J. C.Newell ,"Electrical impedance tomography." SIAM Rev.1999, 32(3), pp.85–101.

[19] B. F. Pedro, A. Felipe, C. Vincence ," High Accurate Howland Current Source: Output Constraints Analysis" Proceedings of the IEEE Circuits and Systems Conference, 2013, 4, pp. 451-458.

[20] Data Sheet, MAX038-High-Frequency Waveform Generator, Maxim Integrated Products, Inc. CA 94086.

[21] Data Sheet, AD829 - High Performance Video Op Amp, Analog Devices, Inc.

[22] T. K.Bera ,J.Nagaraju, "A Study of Practical Biological Phantoms with Simple Instrumentation for Electrical Impedance Tomography (EIT).", Proceedings of IEEE International Instrumentation and Measurement Technology Conference (I2MTC2009), Singapore, 5th - 7th May 2009, pp 511-516.

[23] Data Sheet, CD4067BE, CMOS analog Multiplexer/Demultiplexer, Texas Instruments.

[24] Data Sheet, LM74, Single Operational Amplifier.

[25] P. Pouliquen, J. Vogelstein and R. Etienne-Cummings, "Practical Considerations for the Use of a Howland Cur-rent Source for Neuron-Stimulation," Proceedings of the IEEE Biomedical Circuits and Systems Conference, Bal-timore, 20-22 November 2008, pp. 33-36.

[26] E. Basham, Z. Yang and W. Liu, "Circuit and Coil DE-SIGN for in-Vitro Magnetic Neural Stimulation Systems," IEEE Transactions on Biomedical Circuits and Systems, , 2009, 3(5) pp. 321-331.

[27] K. Sooksood, T. Stieglitz and M. Ortmanns, "An Active Approach for Charge Balancing in Functional Electrical Stimulation," IEEE Transactions on Biomedical Circuits and Systems, 2010, 4(3) pp. 162-170.